Hasanisadi, Mohammadhesam; Tarzamni, Hadi; Tahami, Farzad

Comprehensive Reliability Assessment of Buck Quasi-Resonant Converter

Published in:
2022 IEEE 20th International Power Electronics and Motion Control Conference, PEMC 2022

DOI:
10.1109/PEMC51159.2022.9962912

Published: 01/01/2022

Document Version
Peer-reviewed accepted author manuscript, also known as Final accepted manuscript or Post-print

Please cite the original version:
Hasanisadi, M., Tarzamni, H., & Tahami, F. (2022). Comprehensive Reliability Assessment of Buck Quasi-Resonant Converter. In *2022 IEEE 20th International Power Electronics and Motion Control Conference, PEMC 2022* (pp. 614-620). (International Power Electronics and Motion Control Conference). IEEE. https://doi.org/10.1109/PEMC51159.2022.9962912

Comprehensive Reliability Assessment of Buck Quasi-Resonant Converter

Mohammadhesam Hasanisadi
Electrical Engineering Department
Sharif University of Technology
Tehran, Iran
mhesam1369@gmail.com

Hadi Tarzamni
Department of Electrical Engineering and Automation, Aalto University
Espoo, Finland
hadi.tarzamni@aalto.fi

Farzad Tahami
Electrical Engineering Department
Sharif University of Technology
Tehran, Iran
tahami@sharif.edu

***Abstract*— This paper explores reliability assessment of various Quasi-Resonant (QR) buck DC-DC converters including zero current/voltage switching and half-wave/full-wave topologies. The impacts of output power, input voltage, output voltage, and time duration on the failure rate of each component are investigated, then overall reliability performance of each converter is evaluated. A detailed comparison is performed in which reliability metric of buck soft switching topologies is compared with each other as well as their parent hard switching topology. Eventually, mean time to failure of the converters is analyzed. This approach provides insightful information for selecting the topology or components for the purpose of designing QR converters. To achieve the reliability of these converters, first, the required equations to evaluate the effective factors on the reliability are obtained. Then reliability metric values are calculated for three cases in each of which a key parameter of the converters varies over a specified range.**

Keywords*—— DC-DC converters, mean time to failure (MTTF), quasi-resonant (QR) converter, reliability assessment.

I. Introduction

Power electronic converters are an essential part of energy conversion systems and have attracted considerable attention in recent years [1]. DC-DC converters, in particular, are of greatest—significance thanks to their application in renewable energies, electric vehicles, high voltage DC (HVDC) transmission and energy storage systems [2]. However, industrial experiences have shown that power converters are the most vulnerable component in such systems [3], [4]. Therefore, their availability and reliability are highly critical for the whole system to function properly. Quasi-resonant (QR) converters, which are formed by adding resonant components to the basic pulse width modulation (PWM) converters, have the advantage of zero current switching (ZCS) or zero voltage switching (ZVS). Thanks to their inherent soft switching, they have the benefit of higher efficiency and lower electromagnetic interference (EMI) [5], [6].

Generally, reliability analysis in power electronics field is performed from three different perspectives in the literature: component level, converter level and system level.

- **Component level:** From the component perspective, semiconductor devices seem to be the most reliability-critical component of a power converter. Therefore, most studies are focused on reliability assessment of such components. In [7], reliability of power semiconductor devices such as Metal-Oxide Semiconductor Field Effect Transistors (MOSFET), Insulated Gate Bipolar Transistors (IGBT) and diodes are evaluated under power cycling test by applying a periodical current to these devices and monitoring their temperature. A real-time strategy to improve the reliability of IGBT modules by means of collector-emitter voltage monitoring is presented in [8]. The reliability of emerging Silicon-Carbide (SiC) MOSFETs is analyzed in [9], [10], and compared to the conventional silicon-based MOSFETs.
- **Converter level:** From the converter point of view, various analytical frameworks have been proposed to evaluate reliability of power converters in general and DC-DC converters in particular. Such frameworks provide meaningful information for optimum selecting and designing power converters. Reliability-driven optimization of LC output filter of a Buck converter is made in [11]. In [12], reliability of a conventional boost converter is evaluated in which the effect of variation of each component's characteristics on the overall system's reliability is investigated. It is shown in [12] that the increase in series resistance of main switch or output capacitance results in degradation of converter's reliability metrics. In [13], [14], [15], [16], comprehensive analyses for reliability assessment of conventional isolated multi-switch, isolated and non-isolated PWM DC-DC converters are presented, respectively.
- **System level:** Power electronic converters are crucial components in power conversion systems. Therefore, their reliability plays an important role in reliability of the whole power conversion system. Several studies have been done from such point of view in [17], [18], [19].

In addition, some literature focused on fault tolerant strategies. A comprehensive survey of general fault diagnosis and fault tolerant strategies is presented in [20], [21]. In particular, some techniques are introduced in [22], [23] for three-phase voltage source inverters and full bridge DC-DC converter, respectively, which are based on adding extra components or interleaving to improve the reliability of the converter.

In this paper, the effect of using resonant switch in replacement of the PWM switch network on reliability performance of the converters is investigated. In addition, the performance of various QR topologies, in terms of reliability and mean time to failure (MTTF), are compared. In the present study, failure rate of each component is calculated according to [24], [25], and overall reliability performance of the various topologies of QR buck converter is evaluated. For this purpose, the effects of various parameters such as the output power (P_o), the input voltage (V_g), the output voltage (V_o), and time duration (t) on the reliability and MTTF of these converters is investigated.

Such analysis provide insight for designers to select the best topology that suits the requirements of their design.

This paper is organized as follows: In section II, operation principles of all four possible configurations of the QR Buck converter is discussed. Then, failure rate of each component and total failure rate of the converter are evaluated in sections III and IV, respectively. Finally, numerical results are presented in section V.

II. Operation Principles

In this paper, among manifold QR converters, the buck converter is chosen to be analyzed. Depending on the resonant switch network, four different topologies for QR-buck converter is possible: half-wave zero current switching (HW-ZCS), full-wave zero current switching (FW-ZCS), half-wave zero voltage switching (HW-ZVS) and full-wave zero voltage switching (FW-ZVS) [26]. Such circuits are illustrated in Fig. 1.

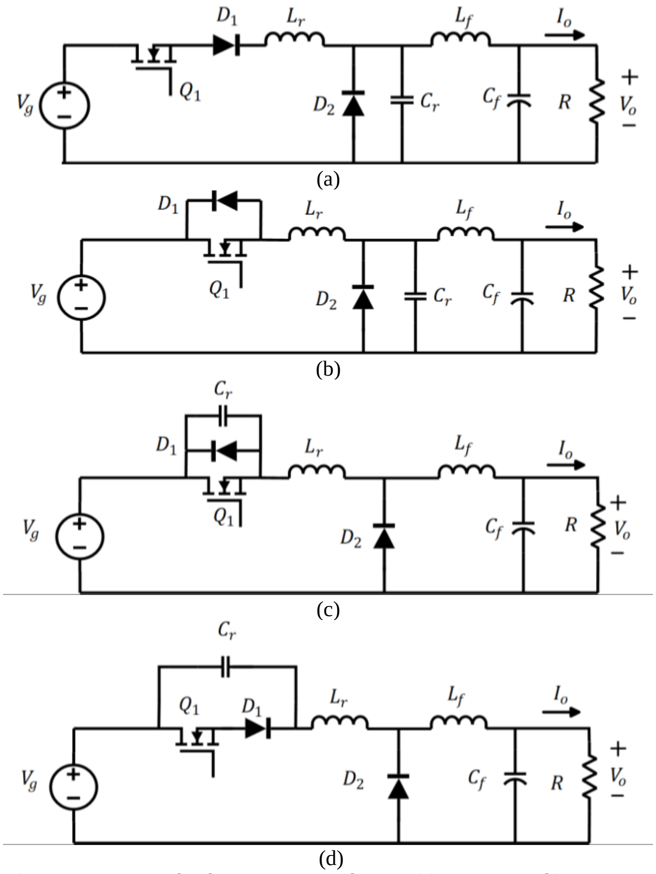

Fig. 1. Various QR buck converter topologies: (a) HW-ZCS, (b) FW-ZCS, (c) HW-ZVS, (d) FW-ZVS.

Based on analytical principles, the mathematical representation and the tank state plane trajectories are simplified considerably when the waveforms are normalized using the base values as expressed in Table I . The normalized switching frequency, output current and output voltage are defined as $F = \frac{f_{sw}}{f_0}$, $M = \frac{V_o}{V_b}$ and $J_T = \frac{I_o}{I_b}$, respectively, where base values are deifned in Table I.

Table I. Base values for normalizing

Base Parameter	Quantity
Base impedance	$R_b = R_0 = \sqrt{Lr/Cr}$
Base voltage	$V_b = V_g$
Base current	$I_b = V_g/R_0$
Resonance frequency	$f_0 = 1/(2\pi\sqrt{L_r C_r})$

The typical waveforms of the QR-Buck converter resonant tank are illustrated in Fig. 2.

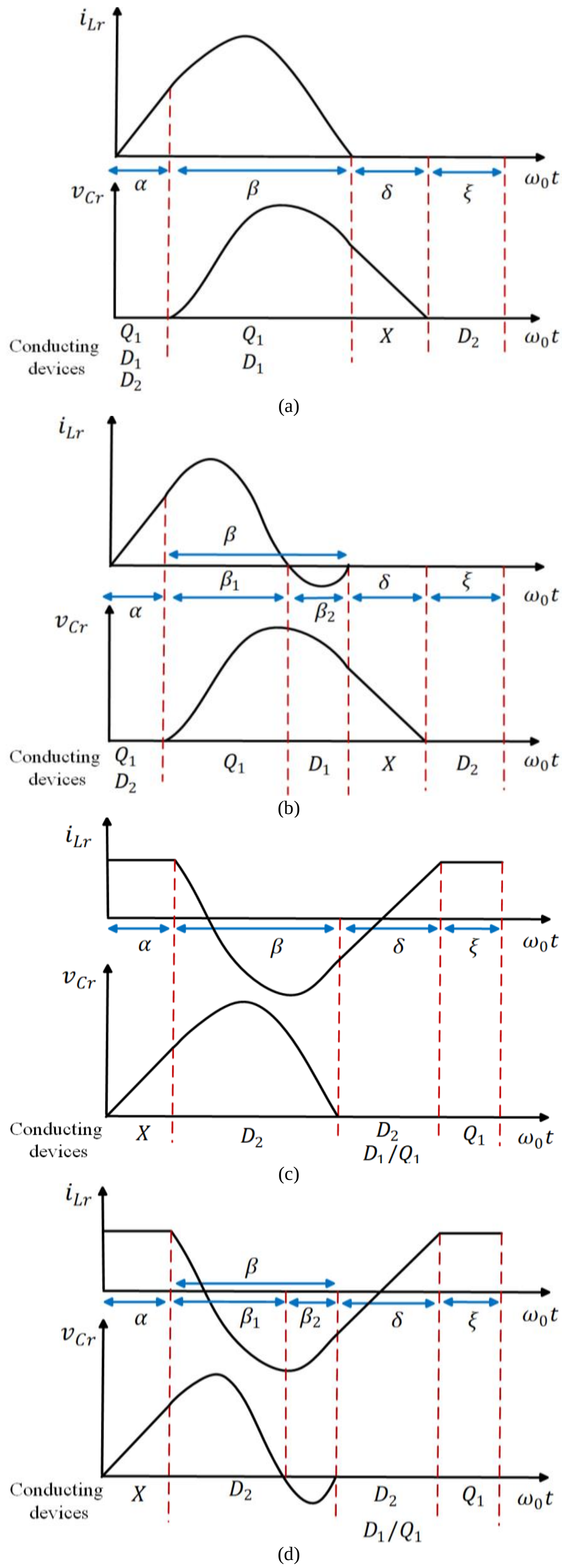

Fig. 2. Typical waveforms of QR buck converter: (a) HW-ZCS, (b) FW-ZCS, (c) HW-ZVS, (d) FW-ZVS.

Depending on Q_1 and D_2 ON or OFF state, four modes are possible for each of QR buck topologies and the angular lengths of the corresponding subintervals are called α, β, δ and ξ which can be expressed as a function of the normalized output current (J_T) in Table II [27].

TABLE II. THE DURATION OF EACH SUBINTERVAL FOR ALL QR BUCK CONVERTERS

	α	β	δ	ξ
HW-ZCS	J_T	$\pi + sin^{-1} J_T$	$\frac{1}{J_T}(1+\sqrt{1-{J_T}^2})$	$\frac{F}{2\pi} - (\alpha+\beta+\delta)$
FW-ZCS	J_T	$2\pi - \sin^{-1} J_T$	$\frac{1}{J_T}(1-\sqrt{1-{J_T}^2})$	$\frac{F}{2\pi} - (\alpha+\beta+\delta)$
HW-ZVS	$\frac{1}{J_T}$	$\pi + \sin^{-1}\frac{1}{J_T}$	$J_T(1+\sqrt{1-\frac{1}{{J_T}^2}})$	$\frac{F}{2\pi} - (\alpha+\beta+\delta)$
FW-ZVS	$\frac{1}{J_T}$	$2\pi - \sin^{-1}\frac{1}{J_T}$	$J_T(1-\sqrt{1-\frac{1}{{J_T}^2}})$	$\frac{F}{2\pi} - (\alpha+\beta+\delta)$

III. FAILURE RATE CALCULATION

Failure rate of a component during its life cycle typically follows the well-known bath-tub curve in which failure rate is constant during useful life-time [28]. With this in mind, failure rate of a component depends on several factors such as material, environmental conditions, quality of manufacturing, operating temperature, voltage stress, etc. which are presented in [24], [25]. In the present paper, such formulas are employed to calculate failure rate of each component. Accordingly, failure rate of each component is evaluated as follows:

$$\lambda_{component} = \lambda_b \prod_{i=1}^{n} \pi_i \ (10^6 \frac{failures}{hour}) \tag{1}$$

where, λ_b is the base value of failure rate, and π_i are factors that influence failure rates including temperature factor (π_T), stress factor (π_S), capacitance factor (π_{CV}), application factor (π_A), quality factor (π_Q), environment factor (π_E) and contact construction factor (π_C). In the following section, failure rate of each type of components is calculated in details.

A. Semiconductor switch

According to [24], failure rate of a MOSFET is evaluated as (2), where $\lambda_b = 0.012$, $\pi_A = 8$, $\pi_Q = 8$ and $\pi_E = 1$. In addition, temperature factor is calculated as (3), where T_{j_Q} is junction temperature of MOSFET, T_a is ambient temperature, $R_{\theta_{JC}}$ and $R_{\theta_{CA}}$ are thermal resistance of junction to case and case to ambient of the switch, respectively. P_Q^{loss} is total loss of MOSFET which is the summation of conducted and switching (P_{sw,Q_1}) losses. The switching loss of a MOSFET for ZCS, ZVS and hard switching configurations can be evaluated as (6), (7) and (8), respectively. In these equations, $R_{DS,on}$ is the drain-source ON resistance, t_{on} is turn-on delay, t_{off} is turn-off delay, and C_{oss} is the output capacitance of MOSFET. Moreover, D is the duty cycle of hard switching buck converter. $I_{rms,Q}$ represents root mean square (RMS) value of switch current which is expressed in Table III.

$$\lambda_{Switch} = \lambda_b \pi_T \pi_A \pi_Q \pi_E \tag{2}$$

$$\pi_T = exp\ (-1925\left(\frac{1}{T_{j-Q}+273} - \frac{1}{298}\right)) \tag{3}$$

$$T_{j\_Q} = T_a + (R_{\theta_{JC}} + R_{\theta_{CA}}) P_Q^{loss} \tag{4}$$

$$P_Q^{loss} = R_{DS,on} {I_{rms,Q}}^2 + P_{sw,Q} \tag{5}$$

$$P_{sw,Q}(ZCS) = \frac{1}{2} f_{sw} (\frac{{V_g}^2}{2L_r} {t_{on}}^2 + C_{oss} {V_g}^2) \tag{6}$$

$$P_{sw,Q}(ZVS) = \frac{1}{2} f_{sw} \frac{{I_o}^2}{C_r} {t_{off}}^2 \tag{7}$$

$$P_{sw,Q}(Hard) = \frac{1}{2} f_{sw} [V_g D I_o (t_{on} + t_{off}) + C_{oss} {V_g}^2] \tag{8}$$

B. Diode

According to [24], failure rate of a diode is calculated as (9); where, $\lambda_b = 0.0038$, $\pi_C = 1$, $\pi_Q = 8$ and $\pi_E = 1$. Temperature factor is calculated as (10), where T_{j_D} is junction temperature of a diode, T_a is ambient temperature, $R_{\theta_{JC}}$ and $R_{\theta_{CA}}$ are thermal resistance of junction to case and case to ambient, respectively. V_S is the stress factor which is defined as the ratio of applied voltage to rated voltage of a diode. Power loss of a diode can be evaluated as (13). $I_{avg,D}$ and $I_{rms,D}$ represent average and RMS value of a diode current, respectively, which are defined in Table III. Forward voltage and resistance of a diode in conducting mode is denoted as V_F and R_D, respectively.

$$\lambda_{Diode} = \lambda_b \pi_T \pi_S \pi_C \pi_Q \pi_E \tag{9}$$

$$\pi_T = exp\ (-3095\left(\frac{1}{T_{j-D}+273} - \frac{1}{298}\right)) \tag{10}$$

$$\pi_S = V_S^{2.43} \tag{11}$$

$$T_{j\_D} = T_a + (R_{\theta_{JC}} + R_{\theta_{CA}}) P_D^{loss} \tag{12}$$

$$P_D^{loss} = V_F I_{avg,D} + R_D {I_{rms,D}}^2 \tag{13}$$

C. Resonant & filter capacitor

Based on [24], failure rate of a capacitor is evaluated as (14), where $\pi_Q = 7$ and $\pi_E = 1$. The base value of failure rate can be calculated as (15) and (16) for resonant and filter capacitor respectively, where S is the stress factor and is defined as the ratio of applied voltage to the rated voltage of capacitor. Furthermore, π_{CV} is the capacitance factor where C is the capacitance in μF.

$$\lambda_{Capacitor} = \lambda_b \pi_{CV} \pi_Q \pi_E \tag{14}$$

$$\lambda_{b-Cr} = 0.0086\left[\left(\frac{S}{0.4}\right)^5 + 1\right] exp(2.5\left(\frac{T_a+273}{358}\right)^{18}) \tag{15}$$

$$\lambda_{b-Cf} = 0.0254\left[\left(\frac{S}{0.5}\right)^3 + 1\right] exp(5.09\left(\frac{T_a+273}{358}\right)^{5}) \tag{16}$$

$$\pi_{CV-Cr} = 1.2C^{0.095} \tag{17}$$

$$\pi_{CV-Cf} = 0.34C^{0.18} \tag{18}$$

TABLE III AVERAGE AND RMS VALUES OF CURRENT FOR RELIABILITY-CRITICAL COMPONENTS OF QR-CONVERTER

	${I_{rms,Q_1}}^2$	I_{avg,D_1}	I_{avg,D_2}	${I_{rms,D_2}}^2$
HW-ZCS	$\frac{F}{2\pi}{I_b}^2\{\frac{{J_T}^3}{3}+\beta {J_T}^2+\frac{\beta}{2}-\frac{\sin 2\beta}{4}+2J_T(1-\cos 2\beta)\}$	$\frac{F}{2\pi}I_b\{\frac{{J_T}^2}{2}+\beta J_T+1-\cos\beta\}$	$\frac{F}{2\pi}I_b\{\frac{{J_T}^2}{2}+\xi J_T\}$	$\frac{F}{2\pi}{I_b}^2\{\frac{{J_T}^3}{3}+\xi {J_T}^2\}$
FW-ZCS	$\frac{F}{2\pi}{I_b}^2\{\frac{{J_T}^3}{3}+\beta {J_T}^2+\frac{\beta}{2}-\frac{\sin 2\beta}{4}+2J_T(1-\cos 2\beta)\}$	$\frac{F}{2\pi}I_b\{J_T(\beta-\beta_1)+\cos\beta\}-\cos\beta_1\}$ $\beta_1=\pi+\sin^{-1}J_T$	$\frac{F}{2\pi}I_b\{\frac{{J_T}^2}{2}+\xi J_T\}$	$\frac{F}{2\pi}{I_b}^2\{\frac{{J_T}^3}{3}+\xi {J_T}^2\}$
HW-ZVS	$\frac{F}{2\pi}{I_b}^2{J_T}^2\{\frac{J_T}{3}+\xi\}$	$\frac{F}{2\pi}I_b\{\frac{{J_T}^2-1}{2}\}$	$\frac{F}{2\pi}I_b\{J_T(\beta-\sin\beta)+\frac{3}{2}\delta^2\}$	$\frac{F}{2\pi}{I_b}^2\{{J_T}^2(\frac{3}{2}\beta-2\sin\beta+\frac{1}{4}\sin 2\beta)+\frac{\delta^3}{3}\}$
FW-ZVS	$\frac{F}{2\pi}{I_b}^2{J_T}^2\{\frac{J_T}{3}+\xi+\frac{\beta_2}{2}-\frac{\beta_1}{2}+\frac{\sin 2\beta_2}{4}-\frac{\sin 2\beta_1}{4}\}$ $\beta_1=\pi+\sin^{-1}\frac{1}{J_T},\beta_2=2\cos^{-1}\frac{1}{J_T}$	$\frac{F}{2\pi}I_b\{1+\xi J_T\}$	$\frac{F}{2\pi}I_b\{J_T(\beta-\sin\beta)+\frac{3}{2}\delta^2\}$	$\frac{F}{2\pi}{I_b}^2\{{J_T}^2(\frac{3}{2}\beta-2\sin\beta+\frac{1}{4}\sin 2\beta)+\frac{\delta^3}{3}\}$
Hard-switching	$D{I_o}^2$	---	$(1-D)I_o$	$(1-D){I_o}^2$

IV. RELIABILITY EVALUATION

Since failure rate of each component in QR buck converter leads to total failure of the system, failure rate of the converter is obtained by adding up the failure rates of components. Hence, considering constant failure rates, failure rate of the converter can be expressed as (19). It is worth mentioning that the case of failure of the inductor is neglected, since the inductor is the component with the lowest failure rate compared to other components. For the power semiconductors, both failure mechanisms, i.e., open circuit and short circuit, result in failure of total converter.

$$\lambda_{total}=\lambda_{Q1}+\lambda_{D1}+\lambda_{D2}+\lambda_{Cr}+\lambda_{Cf} \tag{19}$$

The reliability of the converter can be defined as (20), where $R(t)$ is the probability that the converter will not fail at time *t*.

$$R(t)=exp\,(-\lambda_{total}t) \tag{20}$$

Furthermore, MTTF metric of the converter is defined as (21), based on [28].

$$MTTF=\int_0^\infty R(t)dt=\frac{1}{\lambda_{total}} \tag{21}$$

V. NUMERICAL RESULTS

In this section, effects of variation in several parameters on the reliability of each converter is analyzed. These parameters include output power, input voltage and output voltage. To obtain numerical results, a QR buck converter with input voltage of 50 V, output voltage of 24 V and output current of 2 A is considered. Design parameters of both topologies are as follow: $L_f=0.5$ mH, $C_f=47$ µF, $L_r=2$ µH and $C_r=75$ nF for ZCS, and $L_r=200$ µH and $C_r=82$ nF for ZVS configurations, respectively. The MOSFET is IXFH60N60X3 with $R_{DS,on}=50\,m\Omega$,. Other parameters of the semiconductors are as follow: $V_{F,D1}=0.9\,V$, $V_{F,D2}=0.7\,V$, $R_D=25\,m\Omega$, $t_{on}=20\,ns$, $t_{off}=100\,ns$ and $C_{oss}=1000\,pF$..

A. Variation of output power

The output voltage and the input voltage of the converter is assumed to be constant, while the load is variable. Since the converter operates in a closed-loop manner, the switching frequency changes to ensure a constant output voltage in the entire range of output power. In the case study, the output current changes from 1 A to 10 A, hence the output power varies from 24 W to 240 W. The effect of the output power variation on the reliability at the time $t=0.5\times10^6$ hours and MTTF metrics of all QR converters along with their hard switching parent is depicted in Fig. 3. It is worth mentioning that both ZVS and ZCS operation for the entire range of the output power is guaranteed.

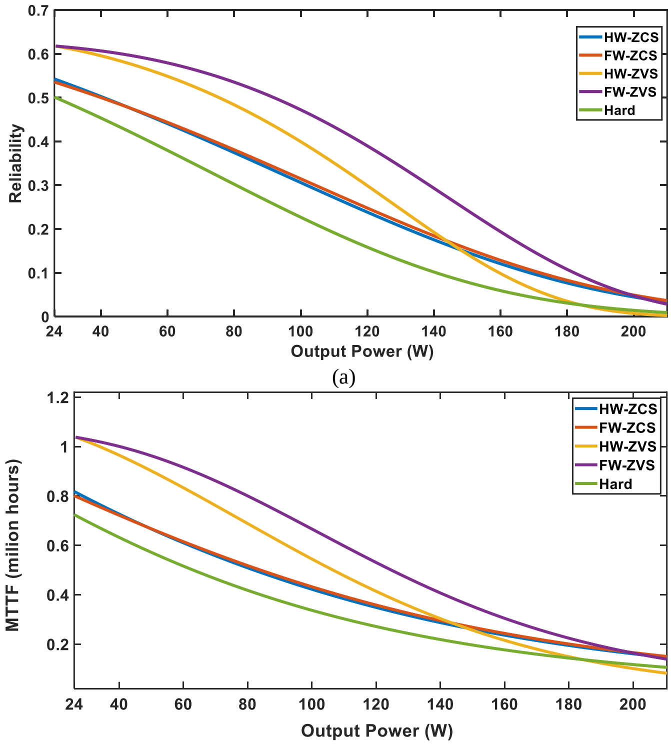

Fig. 3. Comparison of hard switching with QR converter with respect to the output power: (a) reliability, (b) MTTF metric.

As it is evident, the reliability and MTTF of the hard switching is less than all of other QR topologies. Therefore, it is inferred that employing soft switching is an effective solution to enhance the reliability of a converter. The most vulnerable component of a switching converter is the semiconductor switch. As stated in Table III, the RMS of currents in HW-ZCS and FW-ZCS converters are the same. As a result, their power loss and reliability performance are approximately equal. It is obvious from Fig. 2 that, in the ZCS configuration, the peak of switch current and the angular lengths of conducting periods (α and β) are considerably greater than those of the ZVS-type converter Therefore, the thermal stress generated by the power loss of ZCS-type converters is greater than the ZVS-type, resulting in better reliability performance of ZVS configurations. To investigate the effect of time duration in this case, a three-dimensional plot of reliability vs. output power and operation time for HW-ZCS & HW-ZVS converter are illustrated in Fig. 4. One can see that, at any given output power, the reliability decreases as time duration increases.

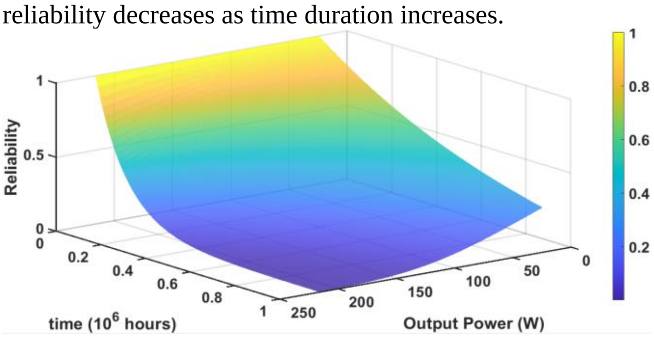

(a)

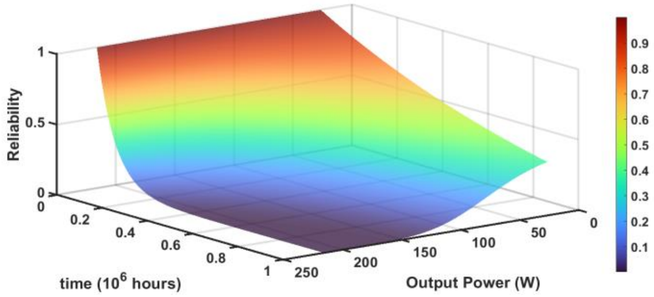

(b)

Fig. 4. Reliability of QR Buck converter with respect to output power and time duration: (a) HW-ZCS, (b) HW-ZVS

B. *Variation of input voltage*

In this section, effect of variation of the input voltage on the reliability and MTTF of QR converter is investigated. The output voltage and the output current are considered constant, and the input voltage varies from 30 V to 100 V. It should be noted that the ZVS and the ZCS are achieved within the entire range of the input voltage. The reliability at the time $t = 0.5 \times 10^6$ hours and MTTF of each converter with respect to the input voltage is shown in Fig. 5.

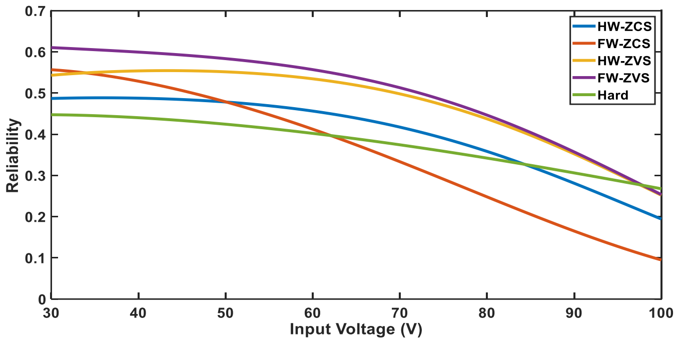

(a)

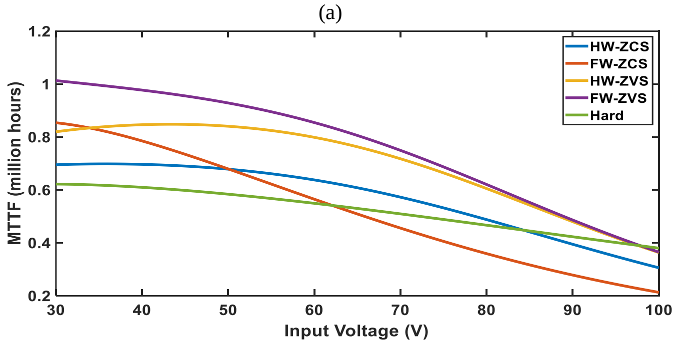

(b)

Fig. 5. Comparison of hard switching with QR converter with respect to the input voltage: (a) reliability, (b) MTTF metric.

In this case, the reliability of hard switching converter is almost independent of input voltage, since the thermal stress for this converter only depends on the output current which is constant in this case. On the other hand, to ensure a constant output voltage, the switching frequency increases as the input voltage goes up resulting in decreased reliability of the converter. Three-dimensional plot of reliability vs. input voltage and operation time for HW-ZCS & HW-ZVS converter ate depicted in Fig. 6.

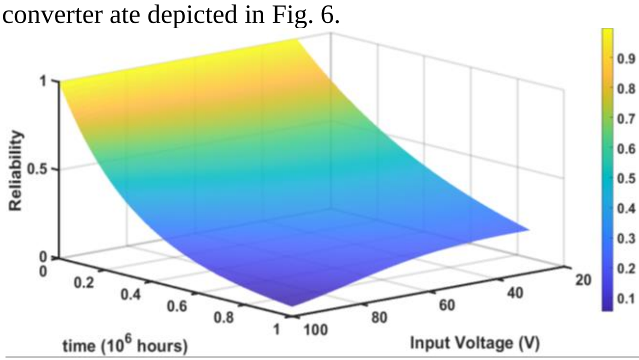

(a)

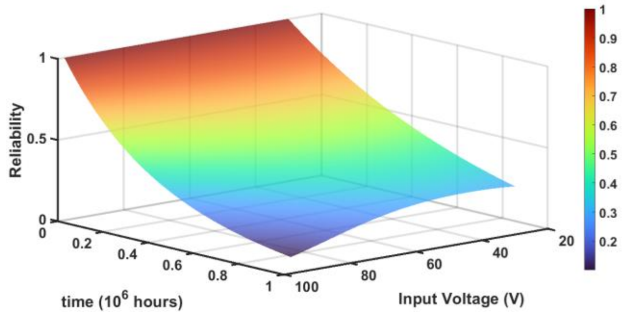

(b)

Fig. 6. Reliability of QR Buck converter with respect to input voltage and time duration: (a) HW-ZCS, (b) HW-ZVS

C. *Variation of output voltage*

In this section, effect of variation of the output voltage on the overall reliability and MTTF of QR converter is analyzed. Input voltage and load resistance is considered constant (50 V and 12 Ω), and the output voltage varies from 12 V to 50 V. Therefore, the output current is variable. In this case, ZVS and ZCS operation is also achieved within the entire range of the output voltage. The reliability at time $t = 0.5 \times 10^6$ hours and MTTF metric of hard switching and soft-switching buck converter is shown in Fig. 7. Similar to the section V, part *A*, the thermal stress caused by power loss on the MOSFET rises as the output voltage increases. Hence, the same implications as section V, part A can be made to compare the reliability of hard and soft switching converter, as well as comparison of various soft switching configurations.

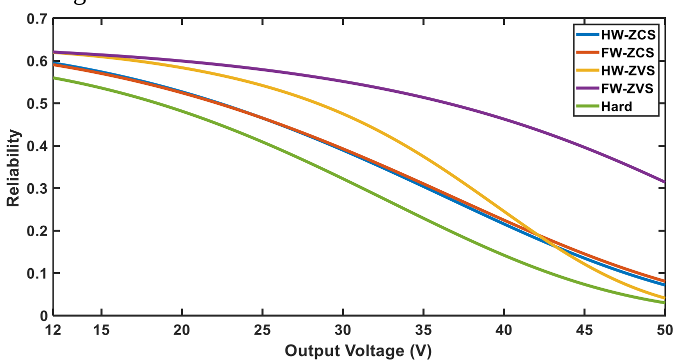

(a)

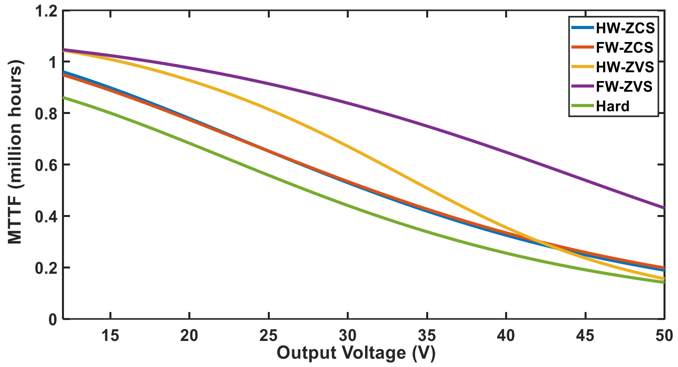

(b)

Fig. 7. Comparison of hard switching with QR converter with respect to the output voltage: (a) reliability, (b) MTTF metric.

By considering both the output voltage and time duration as variable factors, three-dimensional plot for reliability of HW-ZCS & HW-ZVS configurations are shown in Fig. 8

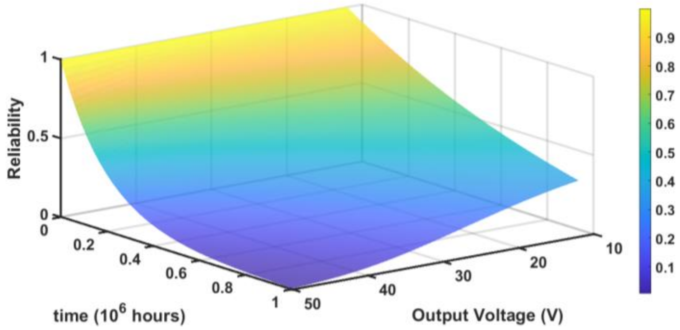

(a)

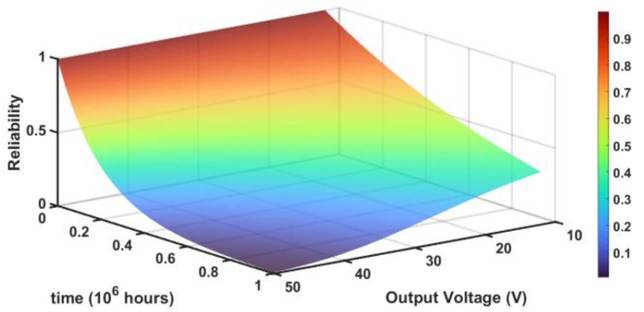

(b)

Fig. 8 Reliability of QR Buck converter with respect to output voltage and time duration: (a) HW-ZCS, (b) HW-ZVS

VI. Conclusion

This paper focused on reliability assessment of the QR buck converter. Numerical analytics are presented to investigate the effect of prevailing factors including output power, input voltage, output voltage and time duration on the reliability and MTTF of these converters. It is concluded that in all of the discussed cases, the hard switching converter is less reliable than QR counterparts. Meanwhile, among various QR converters and under the same circumstances, ZVS configurations are more reliable than ZCS peers thanks to less power loss on the semiconductor switch during the ON state.

VII. References

[1] E. Babaei, H. Tarzamni, F. Tahami, H. K. Jahan, and M. B. B. Sharifian, “Multi-input high step-up inverter with soft-switching capability, applicable in photovoltaic systems,” *IET Power Electron.*, vol. 13, no. 1, pp. 133-143, Jan. 2020.

[2] H. Tarzamni, P. Kolahian and M. Sabahi, “High Step-Up DC–DC Converter with Efficient Inductive Utilization,” *IEEE Transactions on Industrial Electronics*, vol. 68, no. 5, pp. 3831-3839, May 2021.

[3] B. Zhang, M. Wang and W. Su, “Reliability Analysis of Power Systems Integrated with High-Penetration of Power Converters,” *IEEE Transactions on Power Systems*, vol. 36, no.3, pp. 1998-2009, May. 2021.

[4] J. Falck, C. Felgemacher, A. Rojko, M. Liserre, and P. Zacharias, “Reliability of Power Electronic Systems: An Industry Perspective,” *IEEE Industrial Electronics Magazine*, vol. 12, no. 2, pp. 24–35, Jun. 2018.

[5] H. Tarzamni, E. Babaei and A. Z. Gharehkoushan, “A Full Soft-Switching ZVZCS Flyback Converter Using an Active Auxiliary Cell,” *IEEE Transactions on Industrial Electronics*, vol. 64, no. 2, pp. 1123-1129, Feb. 2017.

[6] H. Tarzamni, E. Babaei, A. Z. Gharehkoushan, M. Sabahi, “Interleaved full ZVZCS DC–DC boost converter: analysis, design, reliability evaluations and experimental results,” *IET Power Electron.*, vol. 10, no. 7, pp. 835-845, June. 2017.

[7] H.S. Chung, H. Wang, F. Blaabjerg and M. Pecht, “Reliability of Power Electronic Converter Systems” 2015.

[8] U. M. Choi, F. Blaabjerg, S. Jorgensen, S. Munk-Nielsen, and B. Rannestad, “Reliability improvement of power converters by means of condition monitoring of IGBT modules,” *IEEE Transactions on Power Electronics*, vol. 32, no. 10, pp. 7990-7997, Oct. 2017.

[9] J. Dai, M. Corfield, A. Harris, K. Paciura, J. O'Brien and C. M.Johnson, “Electrical Performance and Reliability Characterization of a SiC MOSFET Power Module with Embedded Decoupling Capacitors,” *IEEE Transactions on Power Electronics*, vol. 33, no. 12, pp. 10594-10601, Dec. 2018.

[10] B. Hu, et. Al, “Failure and Reliability Analysis of a SiC Power Module Based on Stress Comparison to a Si Device,” *IEEE Transactions on Device and Materials Reliability*, vol. 17, no. 4, pp. 727-737, Dec. 2017.

[11] Y. Liu, M. Huang, H. Wang, X. Zha, J. Gong and J. Sun, “Reliability-Oriented Optimization of the LC Filter in a Buck DC-DC Converter,” *IEEE Trans. Power Electron.*, vol. 32, no. 8, pp. 6323-6337, Aug. 2017.

[12] M. K. Alam and F. H. Khan, “Reliability Analysis and Performance Degradation of a Boost Converter,” *IEEE Trans. Ind. Appl.*, vol. 50, no. 6, pp. 3986-3994, Dec. 2014.

[13] H. Tarzamni, F. P. Esmaeelnia, M. Fotuhi-Firuzabad, F. Tahami, S. Tohidi, and P. Dehghanian, “Comprehensive analytics for reliability evaluation of conventional isolated multiswitch PWM DC-DC converters,” *IEEE Trans. Power Electron*., vol. 35, no. 5, pp. 5254-5266, May 2020.

[14] H. Tarzamni, F. Tahami, M. Fotuhi-Firuzabad and F. Blaabjerg, “Improved Markov Model for Reliability Assessment of Isolated Multiple-Switch PWM DC-DC Converters,” *IEEE Access*, vol. 9, pp. 33666-33674, 2021.

[15] H. Tarzamni et al., “Reliability Assessment of Conventional Isolated PWM DC-DC Converters,” *IEEE Access*, vol. 9, pp. 46191-46200, 2021.

[16] H. Tarzamni, F. P. Esmaeelnia, F. Tahami, M. Fotuhi-Firuzabad, S. Tohidi, P. Dehghanian, M. Lehtonen, “Thermal analysis of non-isolated conventional PWM-based DC–DC converters with reliability consideration,” *IET Power Electron*., vol. 35, no. 5, pp. 5254-5266, May 2020.

[17] D. Zhou; H. Wang and F. Blaabjerg, “Mission Profile Based System-Level Reliability Analysis of DC/DC Converters for a Backup Power Application,” *IEEE Transactions on Power Electronics*, vol. 33, no. 9, pp. 8030-8039, Sep. 2018.

[18] S. Yang, A. Bryant, P. Mawby, D. Xiang, L. Ran and P. Tavner, “An Industry-Based Survey of Reliability in Power Electronic Converters,” *IEEE Transactions on Industry Applications*, vol. 47, no. 13, pp. 1441-1451, Jun. 2011.

[19] Y. Song and B. Wang, “Survey on Reliability of Power Electronic Systems,” *IEEE Transactions on Power Electronics.*, vol. 28, no. 1, pp. 591–604, Jan. 2013.

[20] Z. Gao, C. Cecati, and S. X. Ding, “A survey of fault diagnosis and fault-tolerant techniques-part I: Fault diagnosis with model-based and signal-based approaches,” *IEEE Transaction on Industrial Electronics*, vol. 62, no. 6, pp. 3757–3767, Jun. 2015.

[21] Z. Gao, C. Cecati, and S. X. Ding, “A survey of fault diagnosis and fault-tolerant techniques-part II: Fault diagnosis with knowledge-based and hybrid/active approaches,” *IEEE Transaction on Industrial Electronics*, vol. 62, no. 6, pp. 3768–3774, Jun. 2015.

[22] B. Mirafzal, “Survey of fault-tolerance techniques for three-phase voltage source inverters,” *IEEE Transaction on Industrial Electronics*, vol. 61, no. 10, pp. 5192–5202, Oct. 2014.

[23] X. Pei, S. Nie, Y. Chen, and Y. Kang, “Open-circuit fault diagnosis and fault-tolerant strategies for full-bridge DC-DC converters,” *IEEE Transactions on Power Electronics*, vol. 27, no. 5, pp. 2550-2565, May 2012.
[24] MIL-HDBK-217F “Military Handbook: Reliability Prediction of Electronic Equipment”, *Department of Defense*, Washington, DC, 2 Dec. 1991.
[25] “Reliability Prediction Models,” Reliability Information Analysis Center, 6000 Flanagan Rd, Suite 3, Utica, NY 13502-1348, RIAC-MIL-HDBK-217Plus, 2006.
[26] I. Batarseh, A. Harb, “Power Electronics: Circuit Analysis and Design”, Springer, 2018.
[27] D. Maksimovic, “Synthesis of PWM and Quasi-Resonant Dc-to-Dc Power Converters,” Ph.D. thesis, California Institute of Technology, January 1989.
[28] R. Billinton, R.N. Allan, “Reliability Evaluation of Enginearing Systems, Concepts and Techniques” Second Edition, *Springer Scince+Business media press*, New York, 1992, 260-306.